Understanding the Magnetic Behaviour of Diluted Magnetic Semiconductors

Kanu[1], Dr. Anil Kumar[2]

[1]Research Scholar, Sunrise University, Alwar, Rajasthan
[2]Research Supervisor, Sunrise University, Alwar, Rajasthan

Abstract

An examination of the exchange interactions and processes that contribute to the magnetic properties of diluted magnetic semiconductors is provided. Specifically, the importance of long-range interactions in II-VI DMS is highlighted. In this study, we report on the outcomes of experimental investigations on the magnetic behavior of diluted magnetic semiconductors. The magnetic characteristics of both are advantageous at low temperatures and high specific heat $Zn_{1-x}Mn_xSe$ and $Zn_{1-x}Mn_xS$ studies be conducted. In this study, we will focus on the physical principles behind the Mn-Mn interaction, the significance of long-range interactions, and how to include them into model computations.

Keywords: DMS, Semiconductors, materials, mechanisms, magnetic.

1. INTRODUCTION

Semi-magnetic materials, also known as Diluted Magnetic Semiconductors (DMS), are a newer kind of material that typically consists of a nonmagnetic host with a regulated percentage of cations replaced by magnetic ions. The link between the two interacting subsystems, the electronic system of the carriers and the (diluted) magnetic system of paramagnetic ions, is directly connected to the fundamentally fascinating and distinctive aspects of DMS that have gained great attention in recent years. II-VI compounds diluted with Mn have been the focus of the majority of research. $Cd_{1-x}Mn_xTe$, $Zn_{1-x}Mn_xTe$, $Hg_{1-x}Mn_xTe$ and corresponding selenides and sulfides although also compounds like $(Cd_{1-x}Mn_x)_2As_3$ and $(Zn_{1-x}Mn_x)_2As_3$ analyzed in depth. DMS with other magnetic ions from transition metals including Fe and Co has also shown promise in recent reports. Recent publications have provided in-depth analyses of the semiconducting and magnetic characteristics of II-VI DMS in particular.

Semiconducting effects were also rather remarkable, with a gigantic Faraday rotation, anomalous and massive magneto-resistance effects, and a considerable band structure alteration in moderate magnetic fields all being seen. Field amplification and polaron production due to carrier-magnetic ion interaction are the general causes of these phenomena.

The magnetic behavior of such systems is a result of the interactions between the magnetic ions, which are often mediated by the carriers. These interactions are often antiferromagnetic (AF) and have a large range (with significant and systematic variations in range depending on covalency or bandgap). At very low concentrations of magnetic ions, a spin-glass phase is seen (Mn^{2+} as well as Fe^{2+} and Co^{2+}) reaching an extreme dilution. It has been observed that AF ordered regimes may occur at greater doses. Due to the often low concentration of carriers (n, $p < 10^{19}$ cm^{-3}), In order to explain the interaction between the magnetic ions, the well-known Ruderman Kittel Kasuya Yoshida (RKKY) interaction, which is proportional to the carrier density, is insufficient. These interactions may be caused by a variety of physical processes, some of which include bands other than those often considered. There are a lot of articles focused on this topic. Recent theoretical studies suggest that super exchange may be the major mechanism for interactions between closest neighbors. Yet, the spin-glass transition in the diluted limit, which is said to be predominantly induced by the long-range element of the exchange interaction, cannot be due to these nearest-neighbor interactions.

DMS's magnetic properties are the topic of this study. For this reason, we decided to investigate the magnetic characteristics of $Zn_{1-x}Mn_xSe$ to a certain extent. Recent reports have shared these preliminary findings. We report susceptibility and specific-heat results over a broad composition range (0.01 x 0.53) and attempt to interpret these data (along with magnetization11 data and high temperature susceptibility) simultaneously on the basis of a single model incorporating short-range and long-range interaction in a random array.

2. LITERATURE REVIEW

Twesha Patel (2014) In this study, we go over the fundamentals of diluted magnetic semiconductors (DMS), also known as semi-magnetic semiconductors, which are alloys with lattices composed of substitutional magnetic elements such as Mn, Co, Cr, etc. DMS permits the investigation of magnetic phenomena in crystals because to its ease of use, simplicity of band structure, and superior magneto-optical and transport capabilities compared to magnetic semiconductors. Since the spin splitting is also controlled by the confinement energy and the size quantization, DMS layers may be incorporated into transistors, quantum wells, and other electro-optical devices using already available semiconductor hetero structure creation processes. For the next generation of spintronic devices, DMSs, which are broad band gap semiconductors (>3eV), may offer an optoelectronic dimension.

Karl W. Böer et al (2018) Paramagnetic ions provide magnetic characteristics to solids. These are either rare earth ions from the lanthanide family or transition metal ions from the iron series, both of which have an uncompleted electronic 3d shell or 4f shell, respectively. While in pure magnetic semiconductors they are a cation, in diluted magnetic semiconductors they are a substitutional alloy on the cation sublattice. Various exchange interactions relate the magnetic moments of the paramagnetic ions. By contrast, double exchange and p-d exchange are more likely to result in ferromagnetism with parallel alignment of the magnetic moments, while super exchange mediated by the p states of anion ligands promotes anti ferromagnetism with antiparallel alignment. If the thermal energy is greater than the exchange energy, magnetic ordering is disrupted. There are essential Curie and Néel temperatures for the transition from the paramagnetic high-temperature range to the magnetically ordered ferromagnetic and antiferromagnetic regimes, respectively.

Akanksha Gupta et al (2020) Metal oxide semiconductor nanostructures with unusual magnetic characteristics have been the focus of intensive research and development over the last several years. Potential options with enhanced command over charge and spin degrees of freedom include dilute magnetic semiconductor oxides (DMSOs). Transparent DMSOs have a large band gap and exhibit induced ferromagnetism due to the presence of a small amount of magnetic 3d cation, which also results in a long-range antiferromagnetic order. Significant work has been done, however creating DMSO with ferromagnetic characteristics above room temperature remains a formidable obstacle. But large band gap materials like TiO2, SnO2, ZnO, and In2O3 (with 3.2 eV, 3.6 eV, 3.2 eV, and 2.92 eV, respectively) may host a wide variety of dopants to create new chemical structures. It is interesting to note that the grain boundary, existence of defects, and oxygen vacancies in these binary oxides, together with a decrease in size, may produce ferromagnetism even at room temperature. This article gives an overview of the structural analysis and magnetic characteristics of DMSOs based on binary metal oxides nanomaterials with different ferromagnetic or paramagnetic dopants, such as Co, V, Fe, and Ni, that have increased ferromagnetic behaviors at ambient temperature.

M. A. Chuev et al (2011) The electrical-transport, magnetic, optical, and structural properties of diluted-magnetic-semiconductor heterostructures based on GaAs are studied experimentally. These heterostructures consist of a Ga1x Inx as quantum well and a Mn delta layer ranging in thickness from 0.5 ML to 1.8 ML, with the two layers separated by a GaAs spacer with a thickness of 3 nm. Electrical transport and the Hall effect, both of which require the movement of holes through a quantum well, exhibit ferromagnetic behavior. They are a hallmark of quantum well carrier spin polarization. Thanks to the use of high-resolution x-ray diffraction and x-ray reflectivity, we have been able to accurately determine the structural-parameter profiles of the quantum well and the Mn delta layer. This proves that Mn atoms are not evenly dispersed in any direction. This observation is suggestive of a model in which the Mn delta layer is partitioned into nanoscale areas with ferromagnetic ordering and paramagnetic regions. Within this context, the heterostructures' magnetic and electrical-transport features are explored.

John F. DiTusa (2016) We take a look back at the previous 10 years of research towards finding and characterizing magnetic semiconducting systems that may work with current silicon technology. The potential function of intermetallic compounds like silicides and germanides as a magnetic semiconducting source of polarized electrons is considered, as is research into transition metal doping of the group IV semiconductors silicon and germanium. Numerous synthetic methods have been developed for the growth of thin films and nanostructures of these materials, and the ensuing structural characteristics, including the crucial problem of uniformity of dopants, are reviewed critically. Additionally, the ensuing magnetic and carrier transport characteristics are discussed.

3. EXPERIMENTAL RESULTS

The samples of $Zn_{1-x}Mn_xSe$ under the influence of a neutral gas using a modified Bridgman technique. For this material, a cubic crystalline structure has been described x < 0.06, polytypic for 0.06 < x < 0.12 and hexagonal for x > 0.12. Prior magneto-optical research on this material indicated no significant impact from polytypism, although modest dispersion of energy gap for x> 0.2 was reported.

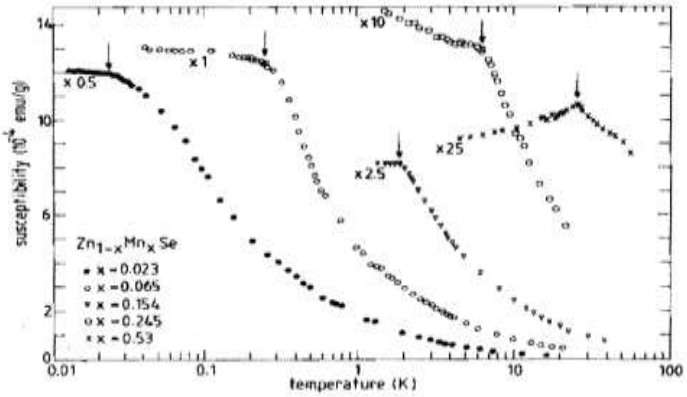

FIG. 1. ac susceptibility of $Zn_{1-x}Mn_xSe$ [x = 0.023, 0.064, 0.154, 0.245 and 0.53 (X)] as a function of temperature for different Mn compositions. The arrows indicate the freezing temperatures T_f. Note the different vertical scales; the data are multiplied by the factor indicated in the figure.

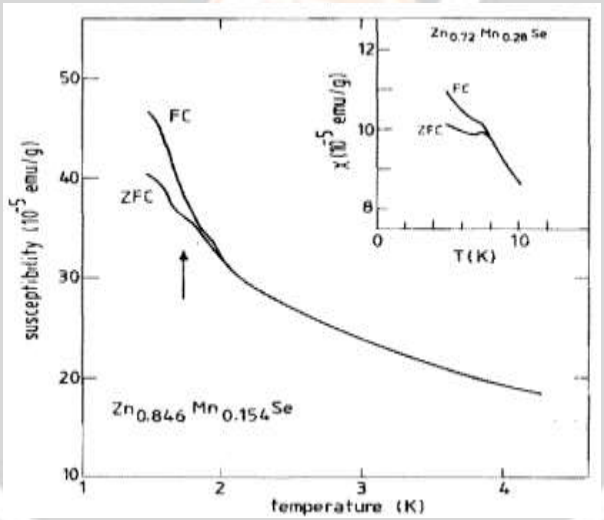

FIG. 2. de susceptibility of $Zn_{0.846}Mn_{0.154}Se$ measured after zero-field cooling (ZFC, H < 1 G) and field cooling (FC, H = 20 G) as a function of temperature. The arrow indicates freezing temperature T_f as obtained from ac susceptibility. Inset: similar data for $Zn_{0.72}Mn_{0.28}$ Se

When determined by microprobe analysis, the Mn concentrations x of the materials under study were: x= 0.014±0.001, 0.023±0.002, 0.056±0.002, 0.064±0.006, 0.103±0.005, 0.154± 0.004, 0.254±0.003 and 0.53±0.02. The real concentrations were generally 50% higher than the theoretical ones used to formulate the recipe.

Low-temperature susceptibility

The ac susceptibility was evaluated by using a standard mutual inductance bridge to examine fields below 1 G in the frequency range 100< f< 2000 f. Equally representative data on sensitivity to x. There may be some variation in the data a.t low temperatures since the findings below 1.5 K were acquired in a dilution refrigerator for which no sufficient absolute calibration of x was available. unusual susceptibility behavior dependent on Mn ion concentration at T_f (freezing temperature) (see Table I).

Extremely high concentrations produce cusp-shaped anomalies, whereas low amounts produce kinked ones. There was an incident similar to this recorded for $Cd_{1-x}Mn_x$- Te where a well-pronounced cusp for x > 0.3 and a kink for x< 0.15 was able to see As we'll see in a little, specific heat shows no signs of weirdness, in contrast to

susceptibility. de Susceptibility Data for Concentrations Above and Below the Percolation Limit, Both Field-Cooled and Zero-Field-Cooled

This signature behavior lends credence to the idea that the susceptibility anomaly represents a phase change to a spin-glass phase. Phase diagram as a consequence, T_f - x, in the range 0.023 ~x~ 0.53. Inspection of this phase diagram shows that T_f+ 0 when x-+ 0. Since no freezing should have been detected for x below the percolation limit, which equates to, this experimental finding suggests that the interactions generating this spin-glass transition are quite long ranging x_c = 0.18 in this case.

TA.BLE 1. The freesing temperature T_f for $Zn_{1-x}Mn_xSe$.

$T_f(x)$	x
0.022	0.023
0.225	0.064
0.55	0.103
1.7	0.154
5.7	0.245
24	0.53

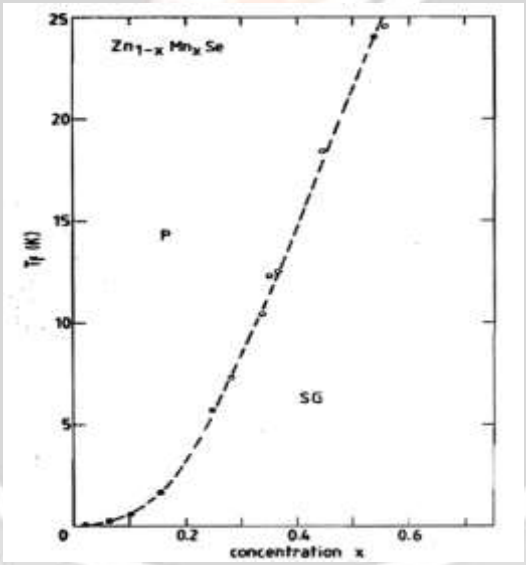

FIG. 3. Phase diagram for $Zn_{1-x}Mn_xSe$. The dashed line is a guide to the eye only.

The ac susceptibility and specific-heat experiments were performed on $Zn_{1-x}Mn_xS$ with x= 0.028, 0.047, 0.092 and 0.097. The microprobe analysis ensured that all concentrations were correct. The susceptibility was evaluated using a 90–9000 Hz, less than 1 G excitation field and a mutual inductance bridge. displays the outcomes at low temperatures. The shift from paramagnetic to spin glass is responsible for the sharp bend in the ac susceptibility. Table I summarizes the freezing point depressions calculated, including some older data for greater concentrations.

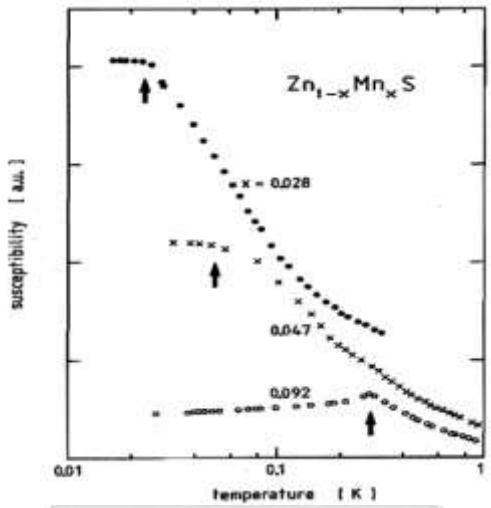

FIG. 4. Low-temperature ac susceptibility of $Zn_{1-x}Mn_xS$; f = 1000 Hz, Hac ≈ 0.5 G. The arrows indicate the freesing temperature T_f.

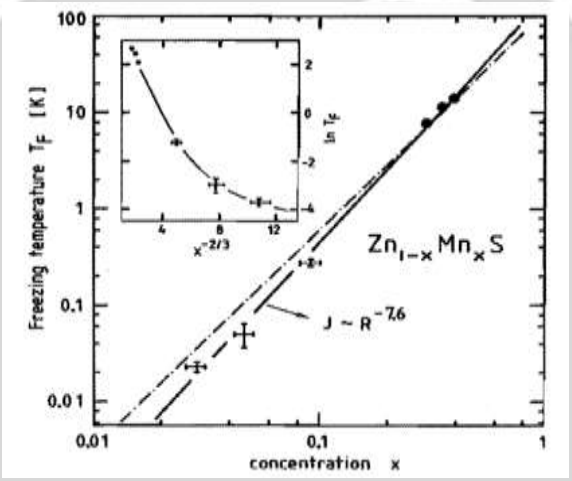

FIG. 5. Freezing temperature T_f of $Zn_{1-x}Mn_xS$ as a function of the Mn concentration x. The full circles are data.

Even in this situation, below the nearest-neighbor (NN) percolation limit, a freezing transition seems to persist to very dilute systems. Earlier, it was mentioned that freezing temperature was a determinant of concentration $T_f(x)$ is connected to the radial dependence of the exchange contact that sets off the shift. With the assumption of power law distribution $J(R) \sim R^{-n}$, $T_f(x)$ can be expressed as

$$\log T_f(x) \sim \tfrac{1}{3} n \log x$$

we plotted T_f versus x, both on a logarithmic scale. The figure shows indeed a linear dependenee between log T_f and logx characterized by n = 7.6. There is a little discrepancy between this finding and those found in related sources like as in which A = Zn,Cd and B = Se, Te, where n is determined to be 6,8 for all systems (indicated by a dashed-dotted curve in Fig). Specific thermal capacity of $Zn_{1-x}Mn_xS$ between 0.4K and 15K using an adiabatic heat-pulse calorimeter. Aspects of magnetism's C_m, found by taking the total specific heat and subtracting the heat generated by the ZnS lattice. The magnetic contribution Cm is just a tiny part of the total specific heat, especially at low concentrations x, which contributes to the dispersion of the data points at higher T. The structure seen in Cm stands out when compared to the specific heat measured in similar compounds. We shall demonstrate that this is because the NN interaction has an exceptionally high value and rapidly decays beyond n = 7.6, leading to clearly distinguishable values for the NN, NNN, and additional magnetic-neighbor interactions.

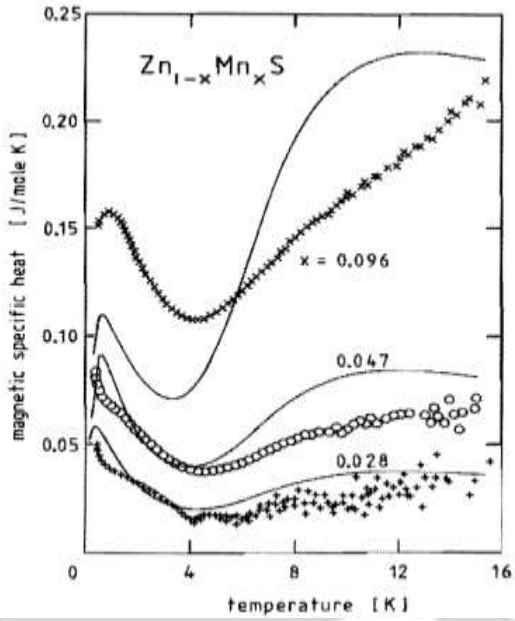

FIG. 6. Magnetic specific heat (Cm) of $Zn_{1-x}Mn_xS$· The solid lines represent the ENNP A calculations with $J_{NN}/k_B = -16$ K and $J(R)/k_B = -10R^{-7.6}$ K.

We have published magnetization (M) and high temperature susceptibility (x) measurements. The thermodynamic and dynamic parameters are consistent with what one would expect from an II-VI wide gap DMS. Examples of magnetization for $Zn_{0.958}Mn_{0.042}S$, shows technical saturation at low temperatures in fields as high as 15 T, much below $M_s = (5/2)g\mu_B$ (≈ 12 emu/g) for paramagnetic ions that have not been linked.

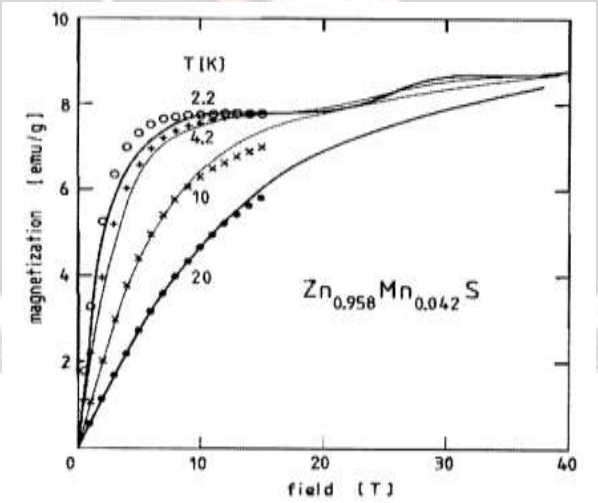

FIG. 7. High-field magnetization {M) of $Zn_{0.958}Mn_{0.042}S$ for several temperatures. The solid lines represent the ENNP A calculations with $J_{NN}/k_B = -16$ K and $J(R)/k_B = -10R^{-7.6}$ K. .

4. DISCUSSION

The influence of the freezing point on concentration was analyzed for $Zn_{1-x}Mn_xSe$ in What was said in the previous paragraph is applicable to other DMS as well. What we can glean from the data we currently have $T_f(x)$ as a large group of them has collected. There always seems to be a description of $T_f(x)$ which is based on a power-law dependence of $J(R) = J_0R$-n matches the data quite well over the whole concentration range, in contrast to the explanation based on an exponential decay of J. (R). However, whether this is suggestive of a particular process remains debatable as (as has been stated) it is not a priori obvious if the same mechanism is responsible for the spin-glass freezing below and beyond the percolation limit.

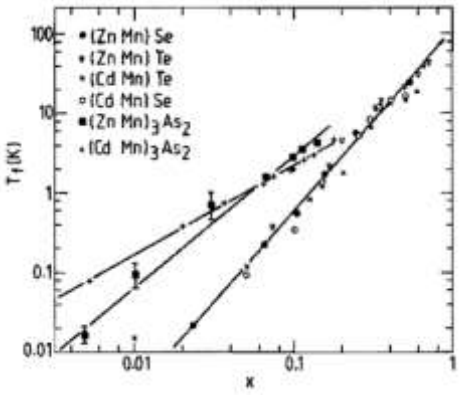

FIG. 8. Freezing temperature T_f as a function of the Mn concentration z for various DMS on logarithmic scale. The straight lines are fitted to the data yielding the power dependence $J(R) \sim R^{-n}$. References on the origin of the data are given in the text.

5. CONCLUSION

In conclusion, based on the previously presented studies, we believe the magnetic characteristics of $Zn_{1-x}Mn_xS$, especially in the diluted limit, may be represented concurrently with a single set of parameters, so long as the long-range character derived from the concentration dependence of the freezing point is taken into consideration. Please note that no tailoring or adjusting has been done in this regard. This method would almost likely lead to a more accurate description of some of the data, but whether or not it would lead to conclusions that have any physical significance is still up for debate.

In this study, we will focus on the physical principles behind the Mn-Mn interaction, the significance of long-range interactions, and how to include them into model computations.

6. REFERENCES:

2. Patel, Twesha. (2014). Diluted Magnetic Semiconductors. 10.13140/RG.2.1.4237.7842.
3. Böer, K.W., Pohl, U.W. (2018). Magnetic Semiconductors. In: Semiconductor Physics. Springer, Cham. https://doi.org/10.1007/978-3-319-69150-3_9
4. Gupta, Akanksha & Zhang, Rui & Kumar, Pramod & Kumar, Vinod & Kumar, Anup. (2020). Nano-Structured Dilute Magnetic Semiconductors for Efficient Spintronics at Room Temperature. Magnetochemistry. 6. 15. 10.3390/magnetochemistry6010015.
5. Chuev, M. & Aronzon, B. & Pashaev, E. & Koval'chuk, M. & Subbotin, I. & Rylkov, V. & Kvardakov, V. & Medvedev, P. & Zvonkov, B. & Vikhrova, O.. (2011). Diluted magnetic semiconductors: Actual structure and magnetic and transport properties. Russian Microelectronics. 37. 73-88. 10.1134/S1063739708020017.
6. DiTusa, J.F. (2016). Si Based Magnetic Semiconductors. In: Xu, Y., Awschalom, D., Nitta, J. (eds) Handbook of Spintronics. Springer, Dordrecht. https://doi.org/10.1007/978-94-007-6892-5_21
7. Cao, H.; Xing, P.; Zhou, W.; Yao, D.; Wu, P. Indium vacancy induced d0 ferromagnetism in Li-doped In2O3 nanoparticles. *J. Magn. Magn. Mater.* **2018**, *451*, 609–613
8. Shen, L.; An, Y.; Cao, D.; Wu, Z.; Liu, J. Room-Temperature Ferromagnetic Enhancement and Crossover of Negative to Positive Magnetoresistance in N-Doped In2O3 Films. *J. Phys. Chem. C* **2017**, *121*, 26499–26506.
9. Kumagai, H.; Hara, Y.; Sato, K. Site occupancy, valence state, and spin state of Co ions in Co-doped In2O3 diluted magnetic semiconductor. *J. Magn. Magn. Mater.* **2019**, 165358
10. Pellicer, E.; Menéndez, E.; Fornell, J.; Nogués, J.; Vantomme, A.; Temst, K.; Sort, J. Mesoporous oxide-diluted magnetic semiconductors prepared by Co implantation in nanocast 3D-ordered In_2O_{3-y} materials. *J. Phys. Chem. C* **2013**, *117*, 17084–17091.
11. Peleckis, G.; Wang, X.; Dou, S. Ferromagnetism in Mn-doped In2O3 oxide. *J. Magn. Magn. Mater.* **2006**, *301*, 308–311
12. Krishna, N.S.; Kaleemulla, S.; Amarendra, G.; Rao, N.M.; Krishnamoorthi, C.; Kuppan, M.; Begam, M.R.; Reddy, D.S.; Omkaram, I. Structural, optical, and magnetic properties of Fe doped In2O3 powders. *Mater. Res. Bull.* **2015**, *61*, 486–491

13. Garnet, N.S.; Ghodsi, V.; Hutfluss, L.N.; Yin, P.; Hegde, M.; Radovanovic, P.V. Probing the role of dopant oxidation state in the magnetism of diluted magnetic oxides using Fe-doped In2O3 and SnO2 nanocrystals. *J. Phys. Chem. C* **2017**, *121*, 1918–1927.
14. Luo, X.; Tseng, L.-T.; Wang, Y.; Bao, N.; Lu, Z.; Ding, X.; Zheng, R.; Du, Y.; Huang, K.; Shu, L. Intrinsic or Interface Clustering-Induced Ferromagnetism in Fe-Doped In2O3-Diluted Magnetic Semiconductors. *ACS Appl. Mater. Interfaces* **2018**, *10*, 22372–22380
15. Baqiah, H.; Ibrahim, N.; Halim, S.; Chen, S.; Lim, K.; Kechik, M.A. Physical properties of Fe doped In2O3 magnetic semiconductor annealed in hydrogen at different temperature. *J. Magn. Magn. Mater.* **2016**, *401*, 102–107.
16. Baqiah, H.; Ibrahim, N.; Halim, S.; Talib, Z.; Flaifel, M.; Abdi, M. Conducting mechanisms and magnetic behaviours of Fe-doped In2O3 nanocrystalline films. *Results Phys.* **2017**, *7*, 1115–1121.